arXiv:astro-ph/0403388v1 16 Mar 2004

O VI, N V, and C IV in the Galactic Halo: I. Velocity-Dependent Ionization Models

Rémy Indebetouw[1] and J. Michael Shull[2]
CASA, Dept. of Astrophysical and Planetary Sciences, University of Colorado, 389 UCB, Boulder, Colorado 80309-0389

ABSTRACT

We explore theoretical models of the ionization ratios of the Li-like absorbers N V, O VI, and C IV, in the Galactic halo. These ions are believed to form in nonequilibrium processes such as shocks, evaporative interfaces, or rapidly cooling gas, all of which trace the dynamics of the interstellar medium. As a useful new diagnostic, we focus on velocity-resolved signatures of several common physical structures: (1) a cooling Galactic fountain flow that rises, cools, and recombines as it returns to the disk; (2) shocks moving toward the observer; (3) a conductive interface with the observer located in the hotter gas. This last geometry occurs with the solar system inside a hot bubble, or when one looks out through the fragmenting top shell of our local bubble blown into the halo as part of the Galactic fountain. In Paper II, these models are compared to ionization-ratio data from FUSE and *Hubble Space Telescope*.

Subject headings: Galaxy: halo — ISM: structure — ultraviolet: ISM

1. Introduction

The nature and dynamics of the interstellar medium (ISM) of galaxies determines how the energy and matter released by stars are redistributed through the universe. It is thus critical to understand the ISM, and in particular that of the Milky Way, which can be observed with greater sensitivity and resolution than other galaxies. The ISM in the disk of our galaxy consists of several phases, from dense and cold molecular gas to hot and fully ionized. Stars heat and disperse the dense clouds in which they form, and that hot gas cools and recombines eventually to complete the cycle and form more stars. It is particularly interesting to consider the interface between this multiphase medium and intergalactic space, where hot gas is released

---

[1] present address: Astronomy Department, University of Wisconsin, 475 N. Charter St, Madison, WI 53706 (remy@astro.wisc.edu)

[2] also at JILA, University of Colorado and National Institute of Standards and Technology (mshull@casa.colorado.edu)

from supernovae to several kiloparsecs in altitude, forming a hot diffuse medium first proposed by Spitzer (1956) as the Galactic corona.

The Galactic corona or halo is almost certainly a dynamic object. It is difficult to construct static halo models, because models supported by thermal pressure are thermally unstable. If conduction is sufficiently important to stabilize small-scale instabilities, then the entire (nearly isothermal) halo is unstable to collapse or expulsion as a wind (see Bregman 1980; Field 1965, for stability arguments). Cosmic-ray supported static halos have been proposed (e.g., Boulares & Cox 1990), but there are considerable uncertainties as to how cosmic rays are confined by the Galaxy (the Galactic magnetic field topology in particular), and these models do not explain the high and intermediate velocity clouds. Considering these things, Shapiro & Field (1976) first proposed a "Galactic fountain" of supernova-heated gas rising buoyantly above the disk until it cools and falls back to the disk. Smooth Galactic fountain models have been constructed by several authors. In particular, Bregman (1980) discussed the issues of radial flow in the Galactic gravitational field for a supersonic hot flow which reaches several kiloparsecs height. More recent models (Houck & Bregman 1990; Breitschwerdt et al. 1993) consist of transsonic flows, which require cooler initial temperatures and only rise to 1–2 kpc. These models can help to explain the population of intermediate velocity halo clouds, believed to exist at those lower heights and velocities compared to the more distant high velocity clouds (e.g., Wakker et al. 1998). The cooling layer certainly fragments into small clouds by Rayleigh-Taylor instability even if no other inhomogeneities exist (e.g., Berry et al. 1998).

Superbubbles, worms, and shell-like structures have been observed in (e.g., Heiles 1984) the upper disk/low halo (few hundred parsecs altitude), but it is difficult to ascertain whether the hot gas is being expelled into the halo. A related issue is the filling factor of hot gas in the disk, which determines the rate at which hot gas can escape into the halo. Estimates for that filling factor and for the rate of reheating by halo supernovae are based on the evolution of supernova remnants in smooth media, but our current understanding of the ISM is increasingly inhomogeneous and dynamic, so those arguments are probably of limited value (Kahn 1998). Recently, the combination of good observations, sophisticated numerical models, and sufficient comprehension of the Galactic fountain may be beginning to allow identification of fountain-like rising structures (de Avillez & Mac Low 2001).

The dynamics of interstellar gas in general and specifically in the Galactic halo may be best understood by studying the hot phase of the ISM (coronal gas at millions of degrees), and gas at temperatures $\sim 10^5$ K intermediate to the hot phase and cooler phases (10^4 K). Of the different interstellar gas phases, the coronal gas is most directly linked to the main sources of energy in the ISM, supernovae and stellar winds. Slightly cooler gas is most closely linked to transient and dynamical processes. This gas is typically short-lived because the cooling time is short at at

10^5 K. The lithium-like ions of common metals, in particular O VI, N V, and C IV, are sensitive tracers of interstellar gas at several times 10^5 K. The resonance absorption lines of these ions are observable with ultraviolet spectrographs on the *Far Ultraviolet Spectroscopic Explorer* (FUSE), and the *Space Telescope Imaging Spectrograph* (STIS) and *Goddard High Resolution Spectrograph* (GHRS) aboard the *Hubble Space Telescope* (HST).

Section 2 describes previous models of high-ion column densities. Section 3 describes new models of the dynamical signatures of the Li-like ions and their interpretation. We summarize in § 4.

2. Previous models of Li-like ions in the dynamic ISM

The ions O VI, N V, and C IV are predicted in models of transient phenomena such as shocks or interfaces between different temperature gas, with conductive heating, turbulent mixing, or rapid radiative cooling (see Spitzer 1996, for a summary). Notable, especially for O VI, is the importance of collisional ionization; by contrast, Si IV is produced in such transient phonomena, but is also commonly produced by photoionization in the Galaxy. The column densities and column density ratios of these high ions can be used to determine which physical scenario is predominant in the ISM. The distributions of C IV and N V in the Galaxy are $(0.6–3)\times10^{13}$ cm^{-2} kpc^{-1} and $(0.5–1)\times10^{13}$ cm^{-2} kpc^{-1} respectively (Savage & Massa 1987). The distribution of O VI is 1–2 regions per kpc, each with a column density of $(2–5)\times10^{13}$ cm^{-2}. These statistics from Shelton & Cox (1994) came from reanalysis of the *Copernicus* dataset presented by Jenkins (1978), who found a higher frequency of lower column-density features. The range in the column density ratio log[N(C IV)/N(O VI)] has been previously measured at -1.5 to -0.5 in the disk and -0.5 to +0.5 in the halo (Spitzer 1996). The values of log[N(N V)/N(O VI)] reported by Sembach et al. (2001b) are -0.4 to -0.9 in the halo, but these represent a small heterogeneous sample of the different lines of sight analyzed by different authors.

The simplest model of gas containing Li-like ions is moderately hot gas in collisional ionization equilibrium (CIE); C IV, N V, and O VI peak in ionization fraction at temperatures of ∼1, 2, and 3×10^5 K, respectively (e.g., Shull & Van Steenberg 1982; Sutherland & Dopita 1993). The ratio between any two species implies a CIE temperature. If derived from two different ion ratios, this CIE temperature does not agree for most real observations of the Galactic halo, indicating that the halo is probably not in collisional ionization equilibrium. This is seen in Figure 1, in which the CIE line ratios lie far to the lower left of more realistic, nonequilibrium models. Although there is some disagreement as to how well atomic abundances are known (Holweger 2001), recent changes in the solar abundances of carbon and oxygen are insufficient to bring these two derived temperatures into agreement, and in fact the latest C/O (Allende Prieto et al. 2002) is very close to older values.

It is important to understand what the predicted ion column density ratios are in more dynamic physical models, beginning with conductive interfaces. Ballet et al.

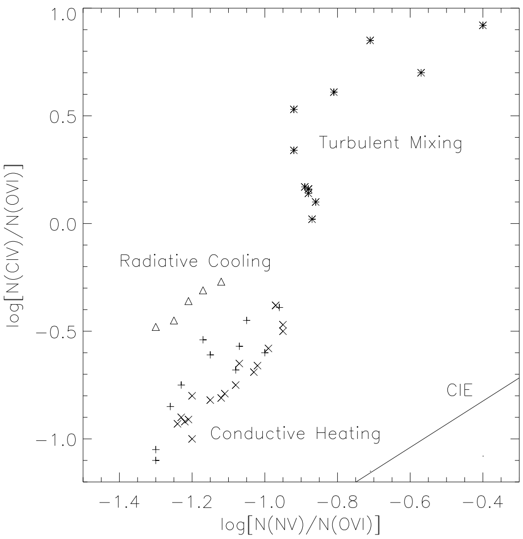

Fig. 1.— Line ratios for various models of high-ion production. The data plotted are from models in the literature: radiative cooling of galactic fountain gas (triangles, Shapiro & Benjamin 1993; Benjamin & Shapiro 1993), turbulent mixing layers (stars, Slavin et al. 1993), and conductive heating and evaporation of spherical, Böhringer & Hartquist (1987) and planar, Borkowski et al. (1990) clouds ("x"s), and in cooling supernova remnant shells (pluses, Slavin & Cox 1993; Shelton 1998). Also shown are the ion ratios for hot gas in collisional ionization equilibrium (Sutherland & Dopita 1993, CIE, solid line,).

(1986) modeled the evaporation of evaporating spherical clouds with nonequilibrium ionization. They presented results for a small ($R = 5$ pc) isolated cloud in a McKee & Ostriker (1977) type model of cool cloudlets in a hot medium of large filling factor. Relative to calculations of evaporation with collisional ionization equilibrium, the total column densities of the Li-like ions is increased, as is the distance from the cloud at which those species reach their maximum abundance. Both effects result from delayed ionization (up to the Li-like ionization stage but especially up to the He-like stage) as the gas is conductively heated. Column densities for all modeled structures are listed in Table 1, and column density ratios are given in Table 2. Böhringer & Hartquist (1987) also modeled evaporating spherical clouds with nonequilibrium ionization, but self-consistently included the effects of radiative cooling on the temperature structure. They found somewhat lower ionization states than Ballet et al. (1986), with higher N V/O VI and C IV/O VI.

Borkowski et al. (1990) presented more sophisticated models of a plane-parallel interface between hot and cold gas. They modeled the time-dependent evolution through an evaporative, steady-state, and recondensation phase. Numbers presented in Tables 1 and 2 are for the longest, steady-state phase, but much higher values of N(N V)/N(O VI) and N(C IV)/N(O VI) are obtained during the initial evaporation, as the species with lower ionization potentials ionize up to the Li-like stages faster. These authors also included a magnetic field, which can suppress thermal conduction if oriented parallel to the in-

Table 1

Li-like ion column densities.

Physical Situation	Si IV (10^{12} cm^{-2})	C IV (10^{12} cm^{-2})	N V (10^{12} cm^{-2})	O VI (10^{12} cm^{-2})	Reference
observed sightlines, kpc^{-1}	2–10[a]	6–30[a]	5–10[a]	10–50[b]	–
evaporating cloudlet	–	1.2–1.5	0.5–0.6	9–12	Ballet et al. (1986)
evaporating cloudlet	.10–.14	2.7–3.8	1.0–1.2	12–14	Böhringer & Hartquist (1987)
planar conduction front	.10–.16	1.6–3.2	.6–1.0	8–10	Borkowski et al. (1990)
planar conduction front	.029–.097	.89–2.7	.40–1.0	6.7–14	Slavin (1989)
stellar wind bubble	.21–.25	3.3–4.0	1.3–1.6	21–25	Weaver et al. (1977)
SNR bubble	.4–.6	6.3–10	3.2–5.0	40–79	Slavin & Cox (1992)
SNR bubble	∼0.52	∼7.8	∼3.6	∼47	Slavin & Cox (1993)
halo SNR bubble	–	8–15	3.4–7.9	35–150	Shelton (1998)
4 $M_\odot$ cooling	3.3–6.4	43–79	28–36	580-600	Edgar & Chevalier (1986)
40 pc cooling cloud	∼25	∼50	∼13	∼200	Benjamin & Shapiro (1993)
turbulent mixing layer	.0010–.47	.025–6.8	.0022–.32	.017–.81	Slavin et al. (1993)
white dwarfs	1.4–4.4	25–77	3.7–12	5.6–20	Dupree & Raymond (1983)

Note.—Predicted column densities vary with physical conditions, for example the temperatures of the hot and cold media in interface models, and an indicative range of column densities is given for each physical model.

[a] Savage & Massa (1987).

[b] Shelton & Cox (1994); Jenkins (1978).

Table 2

Li-like ion ratios.

Physical Situation	$\log\left[\frac{\mathrm{N(C\ IV)}}{\mathrm{N(O\ VI)}}\right]$	$\log\left[\frac{\mathrm{N(N\ V)}}{\mathrm{N(O\ VI)}}\right]$	Reference
observed halo sightlines	-0.5 to +0.5	-0.4 t -0.9	Spitzer (1996); Sembach et al. (2001b)
evaporating cloudlet	-0.95	-1.35	Ballet et al. (1986)
evaporating cloudlet	-0.60	-1.07	Böhringer & Hartquist (1987)
planar conduction front	-0.4 to -0.8	-0.9 to -1.1	Borkowski et al. (1990)
planar conduction front	-0.7 to -0.9	-1.1 to -1.2	Slavin (1989)
stellar wind bubble	-0.8	-1.2	Weaver et al. (1977)
SNR bubble	-0.8 to -0.9	-1.1 to -1.2	Slavin & Cox (1992)
SNR bubble	∼-0.8	∼-1.1	Slavin & Cox (1993)
halo SNR bubble	-0.6 to -1.1	-0.9 to -1.2	Shelton (1998)
4 $M_\odot$ cooling	-0.88 to -1.1	-1.2 to -1.3	Edgar & Chevalier (1986)
40 pc cooling cloud	-0.4 to -0.5[a]	-1.2 to -1.4	Benjamin & Shapiro (1993)
turbulent mixing layers	+0.1 to +0.9	-0.4 to -0.9	Slavin et al. (1993)
WD Strömgren spheres	+0.6 to +0.7	-0.18 to -0.22	Dupree & Raymond (1983)

[a] Much lower C IV/O VI ratios (~ -1.7 in log) are present in the 10^6 K gas before it rapidly cools, but the cooler, overionized stage is much longer lived.

terface. The total column densities of all species are lower in this case, but the N(C IV)/N(O VI) and N(N V)/N(O VI) ratios also decrease, because the evaporated gas is hotter, and the overall ionization state of the front is increased. This effect was confirmed quantitatively by Slavin (1989).

Weaver et al. (1977) modeled a conductive interface of a different kind, at the shell of a wind-blown bubble around a massive star. The hot gas on the bubble interior evaporates the cooler shell that forms around the structure after the swept-up gas is sufficiently dense to cool. Slavin & Cox (1992) performed a similar calculation for a SNR bubble and found higher total column densities, as expected for that more energetic phenomenon, but nearly the same ion ratios, as expected for the same physics. Slavin & Cox (1993) explored the same type of models in more detail and obtained similar results, with scaling laws. Finally, Shelton (1998) extended these SNR models and applied them to a halo with a lower ratio of thermal to nonthermal pressure. She found a variation of the column densities and their ratios with time as the remnant evolves, with a significant decline in the ionization state after 10^7 years, as the shell slows down and the interior cools.

Edgar & Chevalier (1986) modeled the nonequilibrium ionization of cooling gas and scaled their results to a Galactic fountain with 4 $M_\odot\ \mathrm{yr}^{-1}$ of cooling matter. More detailed models of cooling gas incorporating radiative self-ionization (Benjamin & Shapiro 1993; Shapiro & Benjamin 1991; Shapiro & Benjamin 1993) have a similar range of Li-like ion production. Slavin et al. (1993) modeled turbulent mixing layers between million degree gas and cooler (10^2–10^4 K) gas. O VI, N V, and C IV are produced both in the cooling, overionized hot gas, and in the heating, underionized cool gas. These models are physically interesting because the topology of the interstellar medium includes many interfaces between hot and cold gas moving at substantial relative velocities. The models can produce a large range of ion column density ratios and generally produce smaller total column densities per interface than the other models. However, a number of the model parameters are unconstrained by the current state of the observations.

Although C IV and Si IV can be produced by photoionization near hot stars and somewhat in the ISM by ambient stellar ionizing radiation and the soft X-ray background (e.g., Cowie et al. 1981; Black et al. 1980), O VI and N V are almost definitely collisionally ionized in the Galactic disk and halo. Nevertheless, there are some models that produce these ions by photoionization near a sufficiently hot source. Dupree & Raymond (1983) found that hydrogen-rich white dwarfs can produce some O VI in their Strömgren spheres and in diffuse regions if the circumstellar medium is patchy. The Li-like ion column densities depend on impact parameter of a line of sight with the Strömgren sphere, and also increase rapidly with increasing average ISM density (values in Table 1 are for $n_H = 0.1$–1.0 cm^{-3}).

Line ratios for model production mechanisms for Li-like ions are plotted in Figure 1. Clearly, measurements of these line ratios can help to distinguish between different models. Additional detail may even be possible – for example, in the conductive interface models of Böhringer & Hartquist (1987) and Borkowski et al. (1990) ("x"s in Figure 1), models with increasing magnetic field suppressing the conduction are located farther to the lower left of the diagram.

It should be noted that the interstellar abundances of the atoms whose ions are being studied here are not well determined. The models presented above are for solar abundances, reported in Cox (2000), mostly from the work of Grevesse et al. (1996), measured in meteorites and in the solar atmosphere. This technique is particularly difficult for C, N, and O. The models given later in this paper build on the models above, and so the implicit metallicities are those of Grevesse et al. (1996). There is the additional uncertainty of whether solar abundances are appropriate for the general interstellar medium: it has been proposed that the Sun may have uncharacteristically high elemental abundances (e.g., Mathis 1996), and that the lower mean abundances in B stars may be more appropriate (Cunha & Lambert 1992, 1994; Holmgren et al. 1990). The recent downward revision of the solar C, N, and O abundances may bring the interstellar standard back closer to solar (Sofia & Meyer 2001; Allende Prieto et al. 2001, 2002). Gas in the Galactic halo in particular has less than solar abundances, although if the hot gas being observed is recently ejected from the disk, it is less clear what adjustment needs to be made. If elements are depleted onto dust grains, this will most significantly affect N(Si IV). It will also somewhat decrease N(C IV), and N(C IV)/N(O VI) (see discussion in Slavin & Cox 1992, in the specific context of conductive interface models).

3. Velocity-Resolved Models of Li-like Ions

The Li-like ions C IV, N V, and O VI are produced in nonequilibrium physical situations, such as shocks, conductive interfaces, and rapidly cooling gas (§ 2). The different ions are generally produced at different flow velocities in the structure, so a viewer looking through such a structure will see trends in the ion column density ratios as a function of line-of-sight velocity. The ratio-velocity signature in relevant physical situations must be considered to properly interpret trends in the data. Such models are presented in the following pages. For conductive interfaces, we took existing models and calculated the velocity signature that would be observed along a sightline passing through the interface. For radiative shocks, we ran the shock code of J. Raymond and calculated the velocity signature. For supernova remnants, we consider the velocity-resolved results previously presented by Shelton (1998). Finally, for a Galactic fountain, we integrated the steady-state equations published by Houck & Bregman (1990), coupled with the recombination code of Benjamin et al. (2001), to determine the ionization structure as a function of line-of-sight velocity.

3.1. Conductive Interface

One of the oldest interface models containing the Li-like ions is that of a conductive interface. Figure 2 shows the log of column density ratios as extracted from the models of Böhringer & Hartquist (1987). We created this figure by extracting the Li-like ion fraction, temperature, outflow velocity, and pressure as a function of radius from their plots and calculating the column density of the Li-like ions at each radius. Then, we integrated the column density over radius, with a parcel of gas at a certain radius modeled in the absorption spectrum as a Gaussian velocity component centered at the outflow velocity at that radius and having the thermal width of the gas at that radius.

Borkowski et al. (1990) present more sophisticated conductive interface models, with time evolution and a magnetic field. Although the authors do not provide spatially resolved ionization information, they note that the thickness of an ionized layer increases with ionization stage, with C IV occupying ∼0.3 pc, N V 1–3 pc, and O VI ∼8 pc. During the initial evaporative phase, the velocity structure shown in their Figure 4 appears similar to the models of Böhringer & Hartquist (1987), and would thus also show a decrease of ionization stage with increasing outward velocity. It is unfortunately not possible to verify this from the limited information presented in Böhringer & Hartquist (1987). During the steady-state and condensing phases, there is flow back from the hot medium, and thus for the longest-lasting phase of the model, increasing ionization towards more negative velocities would apparently still be observed. From the point of view of an observer in the cool cloud, N(C IV)/N(O VI) and N(N V)/N(O VI) would increase towards more positive velocities as in the Böhringer & Hartquist (1987) models, but

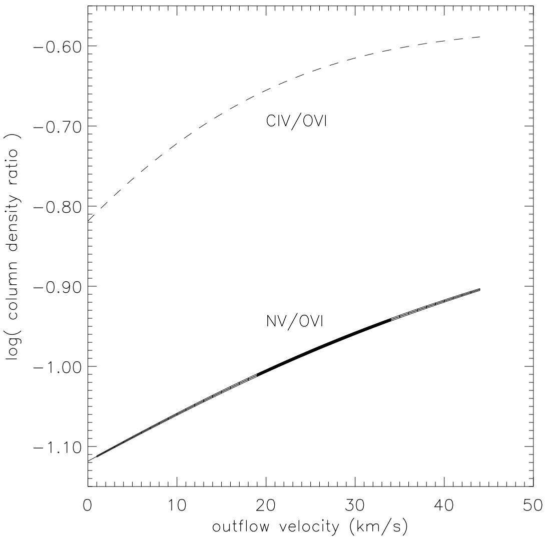

Fig. 2.— Column-density ratio as a function of outflow velocity calculated from the model of Böhringer & Hartquist (1987) of an evaporating cold cloud in a hot medium. An observer in the cool cloud would see this ion ratio spectrum, with positive velocities moving away from the observer. The thickness of the N V/O VI line scales with the density at that point in the flow. Of the sightlines in this study with all three ions, some have N V/O VI profiles that can be explained by a conductive interface, but the models predict lower C IV/O VI than observed.

the absorption would be seen at overall negative velocities. Naturally the situation is reversed for an observer in the hot medium.

An interesting note is that the models of Borkowski et al. (1990) predict increasing linewidths with ionization potential. Linewidths are primarily thermal, and the mean temperature at which a certain ion is found increases with ionization potential. The effect is much more pronouced (∼25% increase in linewidth) from C IV to N V than from N V to O VI (∼4% increase). The observations of Savage et al. (1995) and Sembach & Savage (1992) note an increase in line width between C IV and N V along sightlines that pass through the disk and halo of the Galaxy. New observations (paper II) also show a hint of downturn in the N(C IV)/N(O VI) ratios in the line wings, consistent with the trend seem by other investigators for narrower C IV linewidths than other Li-like ions. No such trend is seen in the N(N V)/N(O VI) ratio, but in conductive interfaces similar to the models of Borkowski et al. (1990) and in gas in collisional ionization equilibrium, the expected linewidth difference is much smaller between N V and O VI than between C IV and O VI.

3.2. Radiative Shock

Shock waves are ubiquitous in the interstellar medium. Of particular interest here are the possible shock at the edge of the local bubble and shocks in a Galactic fountain flow. The latter could arise on the way up, either in the tops of supershells that are bursting out of the disk, oblique shocks in more complicated structures which are breaking out, or on the way down, with condensed clouds reshocking against the diffuse halo as they return to the disk. There is evidence of O VI in high velocity clouds (HVCs), which could result from shocking as they fall through the halo. However, if the halo is close to the virial temperature, then the Mach number of the HVCs is only $M_s \sim 1.2$–1.5, marginally high enough to shock ionize up to O VI.

Figure 3 shows the structure of a 200 km s^{-1} radiative shock, which we calculated using the Raymond shock code (J. Raymond, private communication 1998, Hartigan et al. 1987). Gas immediately behind the shock is highly underionized compared to its high temperature. Cooling is slow above a few million degrees and the gas ionizes up. Further behind the shock rapid cooling takes place and the gas recombines back through the various stages. There is thus a secondary rise in Li-like ions in the cooling zone, the degree of which depends on how much of the He-like ions were produced, which depends on the shock velocity and the metallicity of the gas. The details of the ionization-velocity structure seen by an observer looking through a shock may change depending on these parameters, but the general trend is the same, because the bulk of the observed Li-like ions are are seen as the gas is ionizing up, and C IV, N V, and O VI are ionized sequentially as the flow velocity slows down. Figure 4 illustrates the ion column density ratio as a function of rest-frame flow velocity, i.e. the line-of-sight velocity seen looking through a shock moving towards the observer. As before, the thickness of the line scales with the density of N V and O VI present along the line of sight, so although there are parts of the shock in the cooling zone in which the column density ratio N(N V)/N(O VI) increases with velocity, in the part of the shock with the largest column of those ions, the ratio is decreasing with velocity. A negative slope of N(N V)/N(O VI) with increasingly positive velocity would be observed in a sightline dominated by a a shock moving towards towards the observer, for example on the front faces of Galactic fountain or high velocity clouds falling back to the disk and being shocked against the diffuse halo gas.

3.3. Supernova Remnant Shell

Another structure which may be particularly relevant to observations of Li-like ions in the Galactic halo is a supernova remnant shell. The tops of superbubble shells may be launched into the halo as partially coherent clouds, and if we are living inside a superbubble, there may be remnants of the top of our shell above us, through which many of the sightlines in this study would pass.

Shelton (1998) modeled evolving supernova remnant (SNR) bubbles expanding in ambient conditions typical of the lower halo. In particular, she presented the velocity-resolved column densities of Li-like ions (her Figure 11). Those values and the column density ratios are shown in Figure 5. Clearly, the ion-ratio profile depends on the stage of evolution of the SNR. At very early stages, the interior of the remnant has not yet ionized past the Li-like stages, so these species are found both behind the shock and in the interior, leading to the double-peaked profile in column density. Later, the ions are found in the

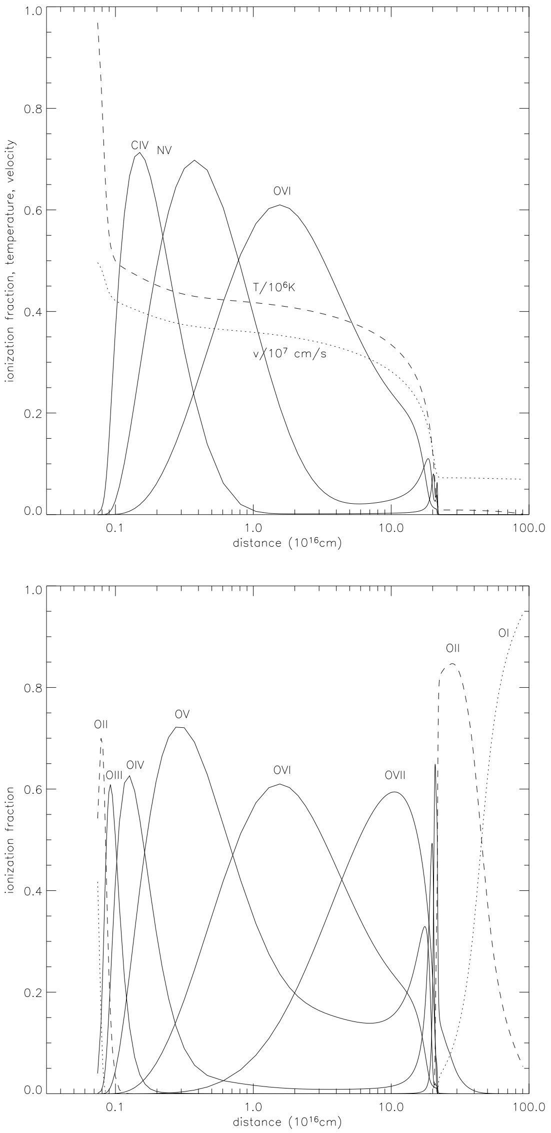

Fig. 3.— Structure of a 200 km s^{-1} interstellar shock, calculated using the Raymond shock code. The first plot shows the Li-like ionization fractions of C, N, and O, the temperature, and the flow velocity as a function of distance behind the shock. The second plot shows the ionization fractions of all stages for oxygen. Intermediate and high ionization stages (e.g., O V here) are present immediately behind the shock as the gas ionizes up, and farther back in the recombination zone, as the gas cools back through $\sim 10^5$ K.

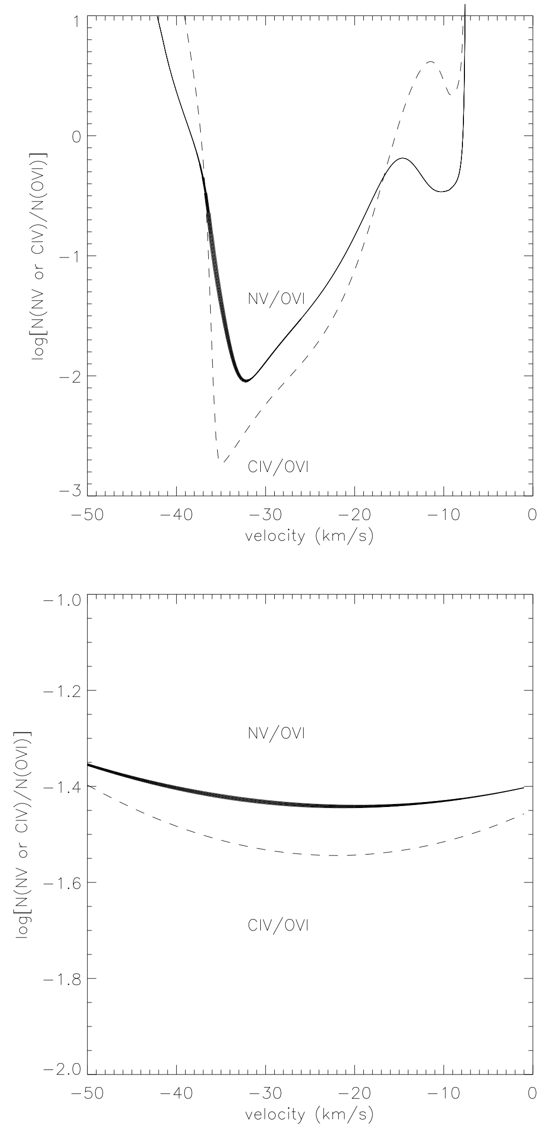

Fig. 4.— Ion column density ratios as a function of flow velocity in a 200 km s^{-1} radiative shock. The thickness of the line scales with the density of N V and O VI present along the line of sight. The first plot shows the column density ratio which would be measured by an observer capable of measuring the volume density *in situ*. The second plot shows what would be measured by an observer using absorption spectroscopy through the shock. The gas at each point in the flow is convolved with the thermal width at that point in the flow, greatly smoothing the observed structure.

cooling but overionized gas at the periphery of the remnant. Finally, as the aged remnant cools, O VI and N V are found mostly in the interior, and C IV near the outskirts.

The profiles of aged remnants are most relevant to the possibility of our looking out through our own superbubble shell, and these profiles show a decrease in N(N V)/N(O VI) with increasing velocity. Additionally, if there is a rising shell above our superbubble, it is probably fragmented owing to Rayleigh-Taylor instabilities as the superbubble blowout expands through the density gradient out of the Galactic disk. Fragmentation and further disturbance by Kelvin-Helmholtz instability, as the shell passes through more stationary diffuse gas, would confuse any velocity-ionization signature. The nature of our local bubble would be better tested with spectroscopy towards stars just outside the local bubble, in which the gas at the bubble interface could be observed independently from other gas which may be involved in different physical processes. The theoretical ion-ratio profiles of remnants at different ages could be very useful for such local bubble observations, or other observations in the disk of the Galaxy which pass through known remnants. If the geometry is well-enough understood, observations of the column density ratio could determine the age of the remnant.

3.4. Galactic Fountain

The nature of a Galactic fountain flow is determined by how the quickly gas cools and recombines as it flows upwards out of the disk. Quantitatively, the comparison is between the cooling time τ_c and the sound crossing time τ_s, which is roughly the time to establish hydrostatic equilibrium:

$$\begin{aligned} \tau_s &= \frac{1}{g}\left(\frac{kT}{\gamma\mu m_p}\right)^{3/2} \\ \text{and} \\ \tau_c &= \frac{nkT}{(\gamma-1)n_e n_H \Lambda(T)}, \end{aligned}$$

where γ is the adiabatic exponent, μ is the atomic weight, and $\Lambda(T)$ is the cooling function (e.g., Houck & Bregman 1990, who discuss the nature of the fountain flow for the different values of τ_s/τ_c). If $\tau_c \gg \tau_s$ then a static system can be established, but it will be unstable to convective overturn and thermal instability (as noted by Bregman 1980, the cooling rate of the static structure is highest at the top of the halo, so clouds will condense out from the top down and be formed with small negative velocities). If $\tau_c \ll \tau_s$ then a supersonic flow will occur. As the gas cools rapidly it is thermally unstable and will condense into clouds which fall out of the flow. The scale height of the gas is then set by the cooling time $H \simeq \tau_c v \simeq \tau_c c_s$, where c_s is the sound speed at the base of the fountain, and clouds can be formed with positive (upward) velocities. For $\tau_c \simeq \tau_s$, transsonic fountain flows exist with clouds forming near the adiabatic density scale height.

Modeling of the velocity-ionization structure of a Galactic fountain will focus here on the transsonic solution ($\tau_s \simeq \tau_c$) of Houck & Bregman (1990). (As discussed below, flow solutions in which the cooling and equilibrium times are very different are not as well-suited to analytic treatment.) Figure 6 shows the structure of the Houck & Bregman (1990) fountain flow, an integration of the one-dimensional steady-state fluid equations, which pass through a sonic point. The equations have the same topology as a standard solar/stellar wind (Parker 1958). The solution stagnates at the top, forming an unphysical dense layer, but in this zone of rapid cooling clouds will condense out with near-zero or small positive vertical velocities and fall back to the disk.

Figure 7 shows the oxygen ionization fractions in a nonequilibrium cooling fountain flow, which we calculated using the nonequilibrium recombination code of Benjamin et al. (2001). We integrated the recombination rate through the temperature and electron density given as a function of time and vertical velocity by the Houck & Bregman (1990) transsonic fountain. It would be slightly more consistent to integrate the fluid equations with Benjamin et al. (2001) nonequilibrium cooling instead of the Edgar (1986) nonequilibrium cooling used by Houck & Bregman (1990), but the differences in the cooling curves are small enough for the combination to be accurate (R. Benjamin, private communication 2001). O VII cannot recombine fast enough as the flow cools rapidly through its collisional ionization equilibrium temperature,$\sim$(5–10)$\times 10^5$ K. Significant O VII remains to low temperatures ($\lesssim 10^5$ K if the density is low enough), until dielectronic recombination allows a recombination cascade. The result is that not only does O VI persist to low temperatures because it is "frozen in" (it cannot recombine fast enough to keep up with cooling), but there can be a *rise* in the O VI fraction as the He-like O VII recombines. This happens for the other Li-like ions N V and

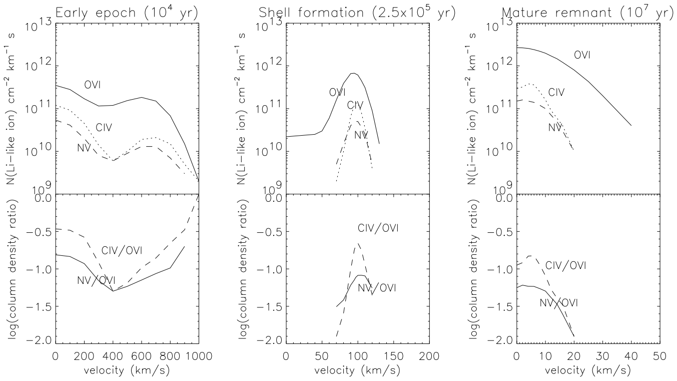

Fig. 5.— Column densities and ratios as a function of velocity for a sightline through the center of a supernova remnant, at various stages of the bubble evolution (Shelton (1998)). The profiles are symmetric about zero velocity, and only positive velocities are shown. Note that the velocity scales change significantly as the shock decelerates.

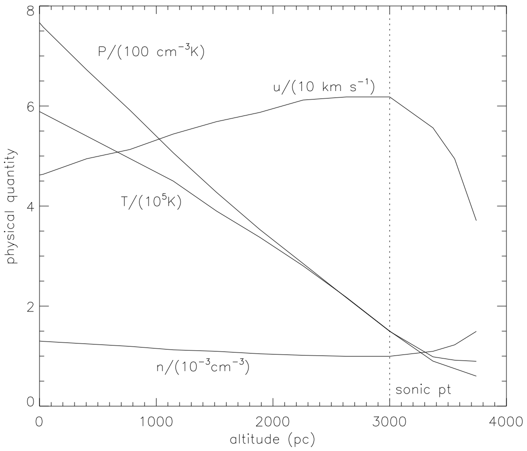

Fig. 6.— Houck & Bregman (1990) transsonic fountain. The vertical dotted line marks the sonic point.

C IV for the same reasons. The magnitude of this effect is dependent on dielectronic recombination rates which have undergone continual revision with time (Benjamin et al. 2001; Shapiro & Moore 1976; Kafatos 1973), and makes the modeling of Li-like ions in cooled ($T{\sim}10^4$ K) clouds uncertain (see discussion and a crude model below).

Figure 8 shows the ion column density ratio calculated by coupling the Benjamin et al. (2001) reionization with the Houck & Bregman (1990) transsonic fountain. The parameters for this particular model are set by choosing the fountain base temperature to be $6{\times}10^5$ K. The two branches in the first plot are a result of the velocity of the fountain accelerating, then decelerating again after passing through the sonic point. The horizontal upper branch is from the rapidly cooled gas at a few 10^4 K, which will condense into clouds and fall out of the flow. The column density of Li-like ions at this point in the flow is highly uncertain, and the column plotted here is probably an overestimate. (R. Benjamin, private communication 2001). The width of the line in the plot scales with the column density of N V and O VI at that point in the flow. Thus, an observation through the fountain is dominated by the rising, cooling gas. The second plot shows the ion column density ratio which would be observed using absorption spectroscopy. Each parcel of gas in the flow was convolved with the thermal width at that point in the flow to create an observed absorption profile, and the ion ratio is calculated from that observed profile. Since the transsonic fountain accelerates, N(N V)/N(O VI) increases with increasingly positive velocity. However, the

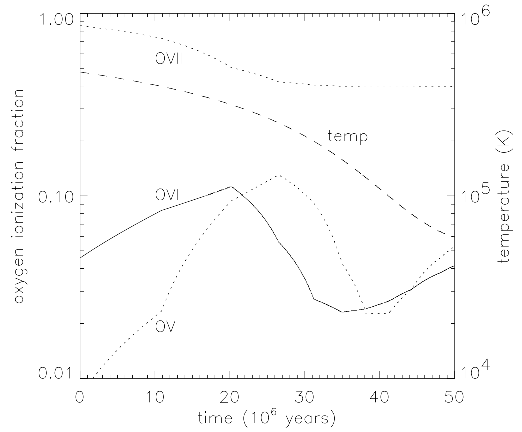

Fig. 7.— Oxygen ionization fractions in a nonequilibrium cooling fountain flow, calculated using the analytical approximation to the hydrodynamic equations of a transsonic fountain of Houck & Bregman (1990) coupled to the ionization code of Benjamin et al. (2001). O VI persists to low temperatures because the gas cools much faster than it can recombine. The O VI ionization fraction can even rise at low temperatures due to the much-delayed recombination of O VII (see text).

trend is very weak due to the small velocity gradient in this fountain model, and it is not clear that the transsonic smooth fountain is a realistic description of the patchy Galactic halo.

It has been noted (de Avillez 2000) that there have been two types of Galactic fountain models in the literature, those with somewhat smoothly distributed rising gas over the disk, as used here, and models that focus on the evolution of superbubbles as the fountain drivers, irregularly spaced in time and galactic location (e.g., Norman & Ikeuchi 1989). Although the latter model is driven differently and rises to larger Galactic altitude than that of Houck & Bregman (1990), the cooling and equilibrium times are still close, the expected spread of velocity in the rising gas is modest, and so the observed ion column density ratio as a function of velocity is probably not qualitatively different from the model considered here. What is needed is an improvement over either type of simple model, i.e. full multidimensional time-dependent models of the fountain with nonequilibrium cooling and nonequilibrium reionization.

Galactic fountain flows in which the cooling and equilibrium times are very different are less well-suited to an analytic treatment because, as discussed above, it is difficult to accurately follow the recombination state of gas which is highly overionized but which has cooled to $\sim 10^4$ K and thermally condensed. In a supersonic fountain ($\tau_c < \tau_s$) clouds condense quickly and observations are dominated by this uncertain cool phase. In a highly subsonic fountain ($\tau_c \gg \tau_s$) there is no velocity signature because the gas rises and establishes

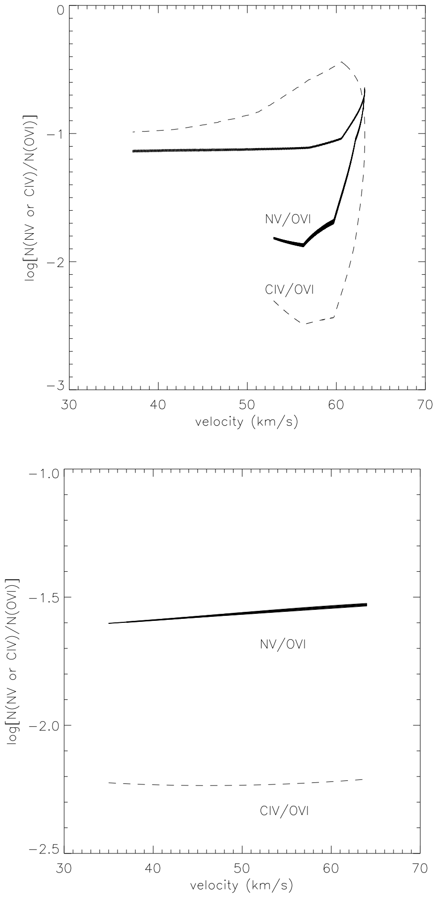

Fig. 8.— Ion column density ratios as a function of velocity for a Houck & Bregman (1990) transsonic fountain coupled to Benjamin et al. (2001) nonequilibrium reionization. The thickness of the line scales with the N V and O VI density along the line of sight, so the observed absorption profile is weighted towards the ratio with the thickest line. For clarity, the column density weighting is only shown for log[N(N V)/N(O VI)]. The first plot shows the ion column density along the flow as it would be measured by an observer in situ capable of measuring the ion volume density at a point in the flow. The second plot shows what the observed ion column density ratio would be for an observed using absorption spectroscopy as was done in this study. The ion column density at each point in the flow is convolved with the thermal width of the gas at the temperature at that point in the flow to create an absorption profile, and the trend is thus significantly smoothed out.

a quasistatic configuration before cooling through the Li-like ions. Any difference in ionization as a function of velocity again occurs in the cold clouds.

Nevertheless, to estimate the behavior of recombination in cool clouds, Figure 9 shows the ion column density ratio as a function of time for a crude model. We consider a cloud formed by thermal instability in a smooth fountain flow at 10^4 K with N V, N VI, O VI, and O VII ionization fractions of 0.06, 0.01, 0.02, and 0.005 respectively. These values are fairly uncertain, and were taken from Shapiro & Moore (1976) with consideration of Benjamin et al. (2001) and Sutherland & Dopita (1993) and the known limitations of these models (R. Benjamin, private communication 2001). The cloud cools slowly at a few $\times 10^4$ K, remaining in pressure equilibrium with the rising smooth hot halo, and thus the density increases, but not by a huge factor. At the same time, hydrogen recombines, so the electron density must decrease. Considering the other large uncertainties of this model, the simple approximation is adequate to allow hydrogen to recombine down to the hydrogen ionization fractions $X_H \sim 0.1 - 0.5$ observed in diffuse halo clouds (Spitzer & Fitzpatrick 1993) and modeled in photoionization equilibrium with ionizing radiation escaping from the Galactic disk (Bland-Hawthorn & Maloney 1999) or old supernova remnants (Slavin et al. 2000). Total (radiative and dielectronic) recombination rates were mostly taken from (Nahar et al. 2000; Nahar 1999; Nahar & Pradhan 1997; Schippers et al. 2001), which shows significant differences from previous work.

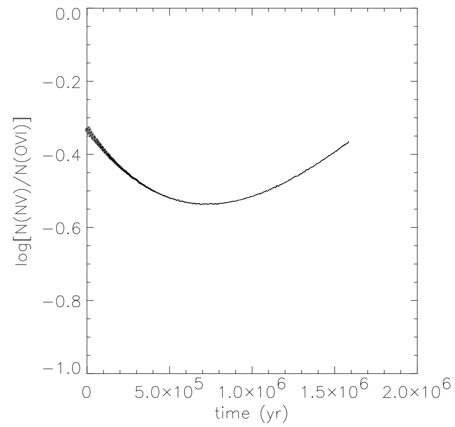

Fig. 9.— Ion column density ratio log[N(N V)/N(O VI)] as a function of time in recombining cool gas. Initial ionization fractions are indicative of what might be found in gas that has rapidly cooled to a few 10^4 K, is highly overionized, and has condensed into a cloud by thermal instability. The exact behavior (for example, the magnitude of the rise relative to the drop in ion ratio) depends on the choice of uncertain recombination coefficients and even more uncertain initial ionization states.

The ion ratio N(N V)/N(O VI) first decreases with time, as the N V total recombination rate is larger than that for O VI. This fact was not true for the older rates of Shull & Van Steenberg (1982). The column density ratio then rises as additional N V and O VI recombine down from N VI and O VII (the recombination rate for the latter is larger). As elsewhere, the thickness of the line in Figure 9 scales with the local density of N V and O VI. The behavior of the ion ratio with time (how much it rises at late times, etc.) varies with the choice of initial ionization fractions, but the recombination time in the cool cloud is always short compared to the return time for the ballistically traveling cloud: the cloud velocity in the Galactic gravitational field ($g \simeq 10^{-8}$ cm s^{-2}) only changes by 3 km s^{-1} in the 10^6 year recombination time. Thus any change in the ionization ratio as a function of velocity determined by the distribution of vertical velocities of clouds at their formation time, not by a slow change in ionization state as the clouds decelerate. The height and vertical velocity of cloud formation depends on the initial temperature of the fountain as discussed above, and simulations show a fairly large spread for a given fountain flow (Bregman 1980). Although the general assertion can be made that clouds recombine as they travel the fountain flow, no conclusions can be drawn about an observable velocity-ionization signature from this type of simple considerations of single clouds. What is needed are full nonequilibrium 3-d simulations of fountain dynamics.

3.5. Other Halo Models

Although the most consistent model of the halo is of a dynamic flow of gas heated and ionized by (thermal) collisions, it is worth considering some of the other physics that could be important and how that might relate to observed Li-like ion column density ratios.

Magnetic fields play a large, but usually neglected, role in interstellar dynamics. For example, the magnetic pressure in the Galactic disk is about the same as the thermal pressure. Synchrotron emission from our Galactic halo and the halos of other Galaxies show that the scale height of the magnetic field is large (Han & Qiao 1994). Dissipation of magnetic energy is a viable mechanism for heating gas to millions of degrees in the disk (Tanuma et al. 2001; Hartquist & Morfill 1984), moderately ionizing and heating diffuse gas in halo (Birk et al. 1998), and even in producing the X-ray emission of boundary regions of high velocity clouds passing through the halo (Zimmer et al. 1997). Raymond (1992) presents a quasistatic halo model in which the gas is heated by magnetic reconnection. The model can produce reasonable column densities of high and moderately ionized species, and reasonable intensities for emission lines of those species. It may have some difficulty fitting both the highly ionized species and the less ionized species, because the lower energy reconnection mechanism which is invoked requires possibly more magnetic power than is available in the Galaxy. In addition, this model would have no kinematic signature, being quasistatic, and the stability of such a model is not discussed in Raymond (1992).

Cosmic rays are another sometimes neglected but important part of the interstellar medium. Again, the cosmic ray pressure in the plane is comparable to the thermal and magnetic pressures. Boulares & Cox (1990) presented a simple static halo supported by cosmic rays (CR), and argued that the stability times are of the order of 10^7 years. More recent work calls into question the stability of CR supported haloes, especially in the presence of CR diffusion which makes CR supported structures more Rayleigh-Taylor unstable (Breitschwerdt et al. 1993). A static CR supported halo would also not have variation of ion column density ratios with line-of-sight velocity. Perhaps more likely is a CR-driven wind, which may operate in parallel with a Galactic fountain, driving material out in regions of open magnetic field topology, while lofted material in regions of closed magnetic field falls can fall back to the disk (Breitschwerdt et al. 1991). These authors concentrate on the CR-driven outflow at hundreds of kiloparsecs from the disk, but their model does have monotonically increasing velocity as gas rises and cools, entrained in the CR wind. The gradient of $\sim$4 km s^{-1} kpc^{-1} is almost identical to that in the lower part of the Houck & Bregman (1990) transsonic fountain, and thus would have a very similar trend of ion column density ratio with velocity. There is the possibility that damping of hydromagnetic waves in the outflow can transfer energy to the gas; the recombination of the gas could be thus delayed to higher altitudes, where the velocity gradient is smaller, and perhaps a steeper change in ion column density ratio as a function of velocity could be produced. To fully understand the Li-like ions in this CR wind, more specific discussion of ionization is required than is provided in Breitschwerdt et al. (1991).

Finally, one can consider that the halo gas is partially photoionized. It has been argued that photoionization is not negligible in the halo (Slavin et al. 2000; Bland-Hawthorn & Maloney 1999), but it is difficult to explain species with large ionization potentials by photoionization, namely N V and O VI. This can be easily shown by calculating the path lengths required to produce the observed N(N V)/N(O VI) column density ratio and simultaneously the total column, or the N(C IV)/N(O VI) ratio. The conclusion is similar for the entire data set: ion column density ratios require high ionization parameters and low space densities, but substantial column densities then require path lengths of tens or even hundreds of kiloparsecs, which is unreasonable to fit in the Galactic halo. In addition, the two ion ratios N(C IV)/N(O VI) and N(N V)/N(O VI) cannot simultaneously fit a photoionization model in most cases. The ionization parameter $U = n_\gamma/n_H$ (n_γ is the number density of hydrogen-ionizing photons) derived from N(C IV)/N(O VI) is about 0.2 dex lower than that derived from N(N V)/N(O VI), indicative of a different (collisional) ionization source.

4. Conclusion and Summary

We have considered the diagnostic power of velocity-resolved column density ratios in understanding the Galactic halo. Column density ratios of Li-like ions in the Galaxy are useful to diagnose the physical formation mechanism of the gas and to study the interstellar gas cycle, and a survey of these ions can reveal general trends. In Paper II, we present a survey of sightlines observed with FUSE and HST, in which the distribution of N(N V) and N(O VI) in the halo does not appear to favor a dominant physical production mechanism.

Here, we have presented models of interfaces and cooling nonequilibrium gas, focusing on the velocity-resolved N(N V)/N(O VI) signatures. In particular, we consider conductive interfaces, radiative shocks and supernova remnants, and cooling gas in a Galactic fountain. Typical ion column density ratios are summarized in Table 3, along with a typical observed slope observed in FUSE and HST data. One important type of hot/cool gas interface for which the ionization-velocity signature has not been discussed is the turbulent mixing layer (Slavin et al. 1993). The structure of these Li-like ion producing structures is uncertain. It is likely that there is a turbulent cascade of eddies which would wash out any velocity-ionization signature, but there may possibly be large Kelvin-Helmholtz rolls with some coherent velocity signature.

The observable velocity-ionization trends are weak, because even very strong trends are washed out by the large thermal width of the gas at different parts of the flow. These trends could be further complicated by thermal instabilities, which likely occur in cooling gas such as in a fountain flow, and can also affect shocks and supernova shells. Fragementation of the gas into parcels with complex density and velocity structure, as seen in the time-dependent shock model of Sutherland et al. (2003) could complicate the signatures described here.

Additional confusion can result when long sightlines pass through multiple structures. As we show in Paper II, the dispersion of N(N V)/N(O VI), both integrated and velocity-resolved, indicates that no single production scenario known to date can completely explain the Galactic halo. To truly understand the physical production of Li-like ions in the halo, one needs to analyze gas in localized areas of physical space, rather than velocity space. Absorption spectroscopy towards many halo stars with close angular separation and different distances could help to isolate gas at a specific altitude. Similarly, the gas above known superbubble shells or chimneys could be isolated. These observations have a greater chance of distinguishing between models of hot gas production than observations along long lines of sight.

We thank S. Penton, E. Wilkinson, J. Green, K. Sembach, and B. Savage for useful discussions. R.I. was partially supported during this investigation by an NSF Graduate Student Fellowship to the University of Colorado. J.M.S. acknowledges support from theoretical astrophysics grants from NASA (NAG5-7262) and NSF (AST02-06042).

Table 3
Summary of models

Model	Slope of Ratio log[N(N V)/N(O VI)]
Radiative shock	$\sim$-0.0015 dex (km s^{-1})$^{-1}$
Mature SNR shell (Shelton 1998)	$\gtrsim$-0.02 dex (km s^{-1})$^{-1}$
Houck & Bregman (1990) fountain	$\sim$+0.002 dex (km s^{-1})$^{-1}$
Indicative observed slope	-0.0032+/-0.0022(r)+/-0.0014(s) dex (km s^{-1})$^{-1}$

Note.—Models
through the structu

REFERENCES

Allende Prieto, C., Lambert, D. L., & Asplund, M. 2001, ApJ, 556, L63

Allende Prieto, C., Lambert, D. L., & Asplund, M. 2001, ApJ, 573, 137

Ballet, J., Arnaud, M., & Rothenflug, R. 1986, A&A, 161, 12

Benjamin, R., & Shapiro, P. 1993, in Ultraviolet and X-ray Spectroscopy of Laboratory and Astrophysical Plasmas, ed. E. Silver & S. Kahn (New York: Cambridge Univ. Press), 280

Benjamin, R. A., Benson, B. A., & Cox, D. P. 2001, ApJ, 554, L225

Berry, D. L., de Avillez, M. A., & Kahn, F. D. 1998, in Lecture Notes in Physics, Vol. 506, The Local Bubble and Beyond, IAU Colloquium No. 166, ed. D. Breitschwerdt, M. J. Freyberg, & J. Trümper (New York: Springer-Verlag), 499

Birk, G. T., Lesch, H., & Neukirch, T. 1998, MNRAS, 296, 165

Black, J. H., Hartmann, L. W., Raymond, J. C., & Dupree, A. K. 1980, ApJ, 239, 502

Bland-Hawthorn, J., & Maloney, P. R. 1999, ApJ, 510, L33

Böhringer, H., & Hartquist, T. W. 1987, MNRAS, 228, 915

Borkowski, K. J., Balbus, S. A., & Fristrom, C. C. 1990, ApJ, 355, 501

Boulares, A. & Cox, D. P. 1990, ApJ, 365, 544

Bregman, J. N. 1980, ApJ, 236, 577

Breitschwerdt, D., McKenzie, J. F., & Voelk, H. J. 1993, A&A, 269, 54

Breitschwerdt, D., Voelk, H. J., & McKenzie, J. F. 1991, A&A, 245, 79

Cowie, L. L., Taylor, W., & York, D. G. 1981, ApJ, 248, 528

Cox, A. N., ed. 2000, Allen's Astrophysical Quantities (AIP Press, Springer-Verlag)

Cunha, K., & Lambert, D. L. 1992, ApJ, 399, 586

—. 1994, ApJ, 426, 170

de Avillez, M. A. 2000, MNRAS, 315, 479

de Avillez, M. A., & Mac Low, M. 2001, ApJ, 551, L57

Dupree, A. K., & Raymond, J. C. 1983, ApJ, 275, L71

Edgar, R. J. 1986, ApJ, 308, 389

Edgar, R. J. & Chevalier, R. A. 1986, ApJ, 310, L27

Field, G. B. 1965, ApJ, 142, 531

Grevesse, N., Noels, A., & Sauval, A. J. 1996, in ASP Conf. Ser. 99: Cosmic Abundances, 117

Han, J. L., & Qiao, G. J. 1994, A&A, 288, 759

Hartigan, P., Raymond, J., & Hartmann, L. 1987, ApJ, 316, 323

Hartquist, T. W., & Morfill, G. E. 1984, ApJ, 287, 194

Heiles, C. 1984, ApJS, 55, 585

Holmgren, D. E., Brown, P. J. F., Dufton, P. L., & Keenan, F. P. 1990, ApJ, 364, 657

Holweger, H. 2001, in AIP Conf. Proc. 598: Joint SOHO/ACE workshop, Solar and Galactic Composition, 23

Hou, J. L., Prantzos, N., & Boissier, S. 2000, A&A, 362, 921

Houck, J. C., & Bregman, J. N. 1990, ApJ, 352, 506

Howk, J. C., Savage, B. D., Sembach, K. R., & Hoopes, C. G. 2002, ApJ, 572, 264

Jenkins, E. B. 1978, ApJ, 220, 107

Kafatos, M. 1973, ApJ, 182, 433

Kahn, F. D. 1998, in Lecture Notes in Physics, Vol. 506, The Local Bubble and Beyond, IAU Colloquium No. 166, ed. D. Breitschwerdt, M. J. Freyberg, & J. Trümper (New York: Springer-Verlag), 483

Mathis, J. S. 1996, ApJ, 472, 643

McKee, C. F., & Ostriker, J. P. 1977, ApJ, 218, 148

Nahar, S. N. 1999, ApJS, 120, 131

Nahar, S. N., & Pradhan, A. K. 1997, ApJS, 111, 339

Nahar, S. N., Pradhan, A. K., & Zhang, H. L. 2000, ApJS, 131, 375

Norman, C. A., & Ikeuchi, S. 1989, ApJ, 345, 372

Parker, E. N. 1958, ApJ, 128, 664

Raymond, J. C. 1992, ApJ, 384, 502

Savage, B. D., & Massa, D. 1987, ApJ, 314, 380

Savage, B. D., Sembach, K. R., & Lu, L. 1997, AJ, 113, 2158

Schippers, S., Müller, A., Gwinner, G., Linkemann, J., Saghiri, A. A., & Wolf, A. 2001, ApJ, 555, 1027

Sembach, K. R., Howk, J. C., Savage, B. D., Shull, J. M., & Oegerle, W. R. 2001b, ApJ, 561, 573

Sembach, K. R., & Savage, B. D. 1992, ApJS, 83, 147

Shapiro, P., & Benjamin, R. 1993, in Star Formation, Galaxies and the Interstellar Medium, ed. J. Franco, F. Ferrini, G. Tenorio-Tagle (New York: Cambridge Univ. Press), 275

Shapiro, P. R., & Benjamin, R. A. 1991, PASP, 103, 923

Shapiro, P. R., & Field, G. B. 1976, ApJ, 205, 762

Shapiro, P. R. & Moore, R. T. 1976, ApJ, 207, 460

Shelton, R. L. 1998, ApJ, 504, 785

Shelton, R. L., & Cox, D. P. 1994, ApJ, 434, 599

Shull, J. M., & Van Steenberg, M. 1982, ApJS, 48, 95 [errata ApJS, 49, 351]

Slavin, J. D. 1989, ApJ, 346, 718

Slavin, J. D., & Cox, D. P. 1992, ApJ, 392, 131

—. 1993, ApJ, 417, 187

Slavin, J. D., McKee, C. F., & Hollenbach, D. J. 2000, ApJ, 541, 218

Slavin, J. D., Shull, J. M., & Begelman, M. C. 1993, ApJ, 407, 83

Sofia, U. J., & Meyer, D. M. 2001, ApJ, 554, L221

Spitzer, L. 1956, ApJ, 124, 20

—. 1996, ApJ, 458, L29

Spitzer, L. J., & Fitzpatrick, E. L. 1993, ApJ, 409, 299

Sutherland, R. S., & Dopita, M. A. 1993, ApJS, 88, 253

Sutherland, R. S., Bicknell, G. V. & Dopita, M. A. 2003, ApJ, 591, 237

Tanuma, S., Yokoyama, T., Kudoh, T., & Shibata, K. 2001, ApJ, 551, 312

Wakker, B., Howk, C., van Woerden, H., Schwarz, U. J., Beers, T. C., Wilhelm, R., Kalberla, P., & Danly, L. 1998, in ASP Conf. Ser. 143: The Scientific Impact of the Goddard High Resolution Spectrograph, 280

Weaver, R., McCray, R., Castor, J., Shapiro, P., & Moore, R. 1977, ApJ, 218, 377

Zimmer, F., Lesch, H., & Birk, G. T. 1997, A&A, 320, 746

This 2-column preprint was prepared with the AAS LaTeX macros v5.2.